

Application of External-Cavity Quantum Cascade Infrared Lasers to Nanosecond Time-Resolved Infrared Spectroscopy of Condensed-Phase Samples Following Pulse Radiolysis

DAVID C. GRILLS,* ANDREW R. COOK, ETSUKO FUJITA, MICHAEL W. GEORGE, JACK M. PRESES, and JAMES F. WISHART

Chemistry Department, Brookhaven National Laboratory, Upton, New York 11973-5000 (D.C.G., A.R.C., E.F., J.M.P., J.F.W.); and School of Chemistry, University of Nottingham, University Park, Nottingham, NG7 2RD, United Kingdom (M.W.G.)

Pulse radiolysis, utilizing short pulses of high-energy electrons from accelerators, is a powerful method for rapidly generating reduced or oxidized species and other free radicals in solution. Combined with fast time-resolved spectroscopic detection (typically in the ultraviolet/visible/near-infrared), it is invaluable for monitoring the reactivity of species subjected to radiolysis on timescales ranging from picoseconds to seconds. However, it is often difficult to identify the transient intermediates definitively due to a lack of structural information in the spectral bands. Time-resolved vibrational spectroscopy offers the structural specificity necessary for mechanistic investigations but has received only limited application in pulse radiolysis experiments. For example, time-resolved infrared (TRIR) spectroscopy has only been applied to a handful of gas-phase studies, limited mainly by several technical challenges. We have exploited recent developments in commercial external-cavity quantum cascade laser (EC-QCL) technology to construct a nanosecond TRIR apparatus that has allowed, for the first time, TRIR spectra to be recorded following pulse radiolysis of condensed-phase samples. Near single-shot sensitivity of $\Delta OD < 1 \times 10^{-3}$ has been achieved, with a response time of < 20 ns. Using two continuous-wave EC-QCLs, the current apparatus covers a probe region from 1890–2084 cm^{-1} , and TRIR spectra are acquired on a point-by-point basis by recording transient absorption decay traces at specific IR wavelengths and combining these to generate spectral time slices. The utility of the apparatus has been demonstrated by monitoring the formation and decay of the one-electron reduced form of the CO_2 reduction catalyst, $[\text{Re}^{\text{I}}(\text{bpy})(\text{CO})_3(\text{CH}_3\text{CN})]^+$, in acetonitrile with nanosecond time resolution following pulse radiolysis. Characteristic red-shifting of the $\nu(\text{CO})$ IR bands confirmed that one-electron reduction of the complex took place. The availability of TRIR detection with high sensitivity opens up a wide range of mechanistic pulse radiolysis investigations that were previously difficult or impossible to perform with transient UV/visible detection.

Index Headings: Nanosecond time-resolved infrared spectroscopy; TRIR; Pulse radiolysis; External-cavity quantum cascade laser; EC-QCL.

INTRODUCTION

The development¹ of flash photolysis in the late 1940s by Norrish and Porter revolutionized the application of fast transient spectroscopic measurements. Modern transient absorption spectroscopy is a technique in which an excitation

source (the pump) initiates a chemical process with a short pulse of energy (e.g., laser light, ionizing radiation, electric discharge, etc.), generating a high concentration of transient species. Continuous-wave probe light passing through the sample at selected wavelengths is used to monitor changes in transmittance that occur after excitation, through the use of a fast detector and a transient digitizer. Depending on the spectral region being probed, this technique allows species with lifetimes as short as a few hundred picoseconds to be interrogated, provided the excitation pulse is short enough. The detection of even shorter-lived transients down to the femtosecond timescale can be achieved using a repetitive sampling technique, with very short excitation and probe pulses and an optical delay line,² or a method to multiplex optical delay measurements.³ Transient absorption spectroscopy has become a very powerful tool for unraveling the kinetics and mechanisms of a wide array of processes, ranging from electron/energy transfer⁴ and solvation/vibrational relaxation dynamics,⁵ to excited state reactivity⁶ and photochemical reactions,⁷ with the most common probe wavelengths being in the ultraviolet (UV)/visible/near-infrared (NIR). However, absorption bands in these regions (particularly in the UV and visible) are often broad and difficult to assign to specific structures of reaction intermediates that would aid in mechanistic interpretation. Time-resolved vibrational spectroscopy (TRVS), with either mid-IR absorption or resonance Raman detection,^{6–8} is a particularly powerful approach since in contrast to the majority of UV/visible measurements, it can provide rich structural information on transient species through the appearance of narrow, highly characteristic spectral bands. Thus, time-resolved infrared (TRIR) and time-resolved resonance Raman (TR³) spectroscopy have become widely used techniques for the identification of short-lived intermediates generated by pulsed laser excitation. Although laser flash photolysis is the most frequently used excitation source for time-resolved measurements, there are many other means of initiating events for investigation by fast spectroscopy. These include rapid mixing with stopped-flow methods,^{9,10} temperature,^{11–13} and pH-jump¹⁴ techniques, and pulse radiolysis.^{15–17}

Pulse radiolysis, utilizing short, high-energy electron pulses from accelerators, is a powerful method for rapidly adding

Received 13 January 2010; accepted 25 February 2010.

* Author to whom correspondence should be sent. E-mail: dcgrills@bnl.gov.

single positive or negative charges to molecules and ions.^{15–17} It is also among the most effective means for creating free radicals. Indeed, there are cases when pulse radiolysis is the only way to initiate a chemical process. For example, molecules lacking any suitable chromophores for laser excitation are conveniently studied by pulse radiolytic methods. Redox-induced processes with metal complexes, in which the photoexcited state of the complex is too short-lived to be quenched by sacrificial electron donors or acceptors, can also only be initiated by pulse radiolysis for time-resolved investigations. Furthermore, even if a redox process can be photoinitiated in the presence of a sacrificial electron donor or acceptor, the resulting oxidized or reduced sacrificial agents may interfere, either chemically or spectroscopically, with the species under investigation; a problem that is often avoided in a pulse radiolysis experiment. The reactions of radicals and redox species generated by pulse radiolysis are important throughout all areas of the chemical and biological sciences in applications as varied as redox catalysis for solar energy utilization,^{18–20} the chemistry associated with advanced nuclear energy systems,²¹ materials for next-generation photovoltaics,²² and studies of DNA damage^{23–25} and other biologically important processes.^{26,27}

In a typical pulse radiolysis experiment on a dilute solution ($[\text{solute}] < 100 \text{ mM}$), the solvent molecules are almost exclusively ionized by the electron pulse, resulting in secondary solvated electrons and various solvent radical species. Depending on the nature of the solvent, and sometimes on the controlled addition of other species to the solution, the overall conditions can be either oxidizing or reducing with varying degrees of oxidizing or reducing potential, allowing precise control of the redox processes that are initiated by the electron pulse.²⁸ However, despite the fact that pulse radiolysis was developed more than 50 years ago,^{29–35} transient detection has been performed mainly by measurement of absorption and emission in the UV/visible/NIR, together with electrical and microwave conductivity, and various magnetic resonance methods such as electron paramagnetic resonance (EPR) and chemically induced dynamic electron polarization (CIDEP).^{15,34,36–41} These approaches can yield excellent kinetic data but often provide little direct information about the structures of the transient species that are being detected.

As mentioned above, vibrational spectroscopy offers the highly specific molecular and structural characterization that is lacking, but has received only limited application in pulse radiolysis. For example, there have been reports of using TR³ methods to study intermediates in pulse radiolysis, most notably at the Risø National Laboratory in Denmark and the Notre Dame Radiation Laboratory in the USA. Examples include TR³ spectroscopy of the triplet states of biological molecules such as β -carotene and *all-trans*-retinal,^{42–44} and various other triplets and radical cations/anions of organic^{45–49} and inorganic species,^{50,51} such as phenylthiyl, various semiquinones, phenoxy, aniline, O₃⁻, and (SCN)₂⁻. However, this approach has several challenges, most notably that (1) resonance conditions are required to obtain satisfactory signal-to-noise; (2) the Raman probe laser may not be innocent, sometimes causing photochemistry; and (3) a large amount of signal averaging is necessary for these measurements, which requires large quantities of sample, particularly when following non-reversible chemical reactions.

In principle, TRIR spectroscopy would be applicable to the study of a much wider range of samples than TR³, particularly since the IR probe light is nondestructive and in certain cases TRIR can prove to be more sensitive than TR³ spectroscopy. However, until now the coupling of TRIR with pulse radiolysis has been limited to only a handful of gas-phase studies. The first of these were pioneering microsecond TRIR measurements by Schwarz, performed over 30 years ago on gas-phase ammoniated ammonium and oxonium hydrate ions generated by pulse radiolysis.^{52,53} In this early work, a globar was used as the IR source with a dispersive IR spectrometer for detection. This was followed by another group in the 1990s that used IR diode-laser-based microsecond TRIR to probe the kinetics of the gas-phase reactions of various small molecules and radicals (e.g., NH₂, CF₃, CH₃, NO, N₂O, and FNO) initiated by pulse radiolysis.^{54–60} However, to the best of our knowledge there have been no reports of pulse radiolysis-TRIR being applied to condensed-phase chemistry, largely due to the many technical challenges associated with such measurements. These include the fact that (1) short path lengths are required for condensed-phase TRIR (usually $\leq 1 \text{ mm}$) due to strong IR absorption by the solvent (resulting in smaller signal sizes), unlike in gas-phase TRIR where path lengths of several meters can be employed; (2) mid-IR detectors are less sensitive than UV/visible/NIR detectors; (3) mid-IR molar absorptivities are normally much smaller than those of UV/visible/NIR bands; (4) the concentration of transient species generated by pulse radiolysis is often much lower than in laser flash photolysis, thus exacerbating the problems highlighted in (1) through (3); (5) water is a commonly used solvent for pulse radiolysis but it absorbs intensely throughout the mid-IR, requiring extremely short path lengths ($< 100 \mu\text{m}$); (6) until recently there has been no high output power continuous-wave (cw) IR source available that is tunable throughout the mid-IR region, and (7) in a pulse radiolysis environment it is often necessary to separate the sample from the detection system by a large distance (several meters) to reduce electromagnetic interference and exposure of the detection system to radiation; the long-distance transport of mid-IR beams is non-trivial due to strong absorptions by atmospheric water vapor and CO₂ in certain regions of the spectrum.

Considering these challenges, it is therefore clear that the routine application of fast (sub-millisecond) TRIR to condensed-phase pulse radiolysis will require high radiolytic dose electron pulses to maximize the concentration of transient species generated, together with the use of high output power IR probe sources. This combination will provide the necessary sensitivity for condensed-phase pulse radiolysis-TRIR measurements, enabling the elucidation of reaction mechanisms that were previously difficult, or even impossible, to follow with UV/visible detection. To the best of our knowledge, the only other group currently making progress toward the application of TRIR spectroscopy to condensed-phase pulse radiolysis is in the CEA Laboratoire de Radiolyse (Saclay, France), where a rapid-scan Fourier transform infrared (FT-IR) based approach is being developed, currently with ~ 20 – 30 s time resolution.^{61,62}

For nanosecond (and longer) time-resolution TRIR measurements, the choice of IR source is typically limited to either a globar or a lead-salt semiconductor IR diode laser. Although very sensitive measurements have been obtained using a globar-based dispersive TRIR spectrometer following UV/

visible excitation,^{63,64} such experiments require extensive signal averaging, which is not amenable to the low repetition rates of typical pulse radiolysis equipment. The CO gas laser was extensively used as an IR laser source in many of the early laser flash photolysis TRIR experiments^{65,66} since it emits with an extremely high output power (up to ~1 W) with a very narrow (essentially monochromatic) linewidth. Thus, it is potentially an ideal probe source for pulse radiolysis-TRIR experiments. However, CO lasers have a limited spectral window in the mid-IR (approximately 1600–2000 cm⁻¹ with a cooled cavity)⁶⁶ and generate TRIR spectra with a fairly low spectral resolution (discrete laser lines tunable in approximately 4 cm⁻¹ steps). Although lead-salt diode lasers are much more versatile in that they are continuously tunable throughout the entire mid-IR,^{7,66} each laser head is restricted to a small region of the mid-IR (≤ 100 cm⁻¹), and their output power is much lower than a CO laser (≤ 1 mW), putting a severe limitation on the signal-to-noise ratio. In addition, they require inconvenient cryogenic cooling for their operation. Despite these limitations, IR diode lasers have become a very common probe source for nanosecond laser flash photolysis-TRIR applications. However, they do not have sufficient output power to extend this versatility to condensed-phase pulse radiolysis. The complementary approach of time-resolved step-scan FT-IR is also a very powerful and commonly used form of TRIR but could be more challenging to couple with pulse radiolysis on the nanosecond timescale, since it uses a global IR source and requires a large number of sample excitation pulses.^{67,68}

The TRIR technique continually advances with new technology and the development of the quantum cascade laser (QCL) now offers such an opportunity.^{69,70} Unlike diode lasers, which emit photons upon electron-hole pair recombination across the material band gap, QCLs are unipolar devices comprising a superlattice formed from a periodic series of thin layers of two different semiconductors of varying material composition that are grown by techniques such as metalorganic chemical vapor deposition (MOCVD). Laser emission is achieved *via* intersubband transitions in the repeated stack of multiple quantum well heterostructures. Thus, rather than being annihilated by electron-hole recombination, as in a traditional diode laser, each electron injected into a QCL's active region cascades down a series of discrete energy levels within the conduction band, emitting a photon at each stage. This cascade effect results in much higher output powers than diode lasers (e.g., up to 100 mW *cf.* < 1 mW for a typical mid-IR diode). The other major advantage of QCLs is that they can be designed to emit at almost any desired wavelength in the mid- and far-IR by changing the thickness of the layers in the heterostructure during the growth process. QCLs also require only moderate thermoelectric cooling and are extremely compact and portable devices.

Until recently, QCLs have been sold as either simple multi-mode Fabry-Pérot lasers (FP-QCLs) or as distributed feedback lasers (DFB-QCLs), in which a grating is etched into the active region to force the operation of the laser at a very specific wavelength determined by the grating periodicity. As a consequence, the DFB-QCL is a single-mode device, operating at a single frequency that may be adjusted only slightly (up to ~ 10 cm⁻¹) by changing the temperature of the active region. This has proved to be extremely useful for high-resolution spectroscopy of trace-gas molecules (e.g., NO, N₂O, CO, NH₃, CH₄ etc.) for a variety of possible applications including

remote atmospheric sensing of environmental gases and pollutants, chemical sensing, and medical diagnostics.⁷¹

Spectroscopic detection techniques have varied from simple direct IR absorption spectroscopy,⁷² to more sophisticated methods such as cavity ringdown spectroscopy,⁷³ cavity-enhanced spectroscopy,⁷⁴ photoacoustic spectroscopy,⁷⁵ and Faraday modulation spectroscopy.⁷⁶ However, performing IR laser spectroscopy on multiple gases simultaneously or on condensed-phase samples, which exhibit much broader absorption bands, requires an IR laser that is widely tunable. Although there has been some application of FP- and DFB-QCLs to the fixed-wavelength analysis of species dissolved in aqueous solution (e.g., sulfite, sulfate, CO₂, glucose, and acetate), demonstrating the utility of high-power QCLs for probing aqueous solutions,^{77–81} these QCLs would not be particularly useful as tunable IR sources for condensed-phase TRIR measurements. **Fortunately, the recent commercialization of external-cavity (EC) technology for QCLs is set to revolutionize the field of IR laser spectroscopy,^{82,83} and we believe it will be the key to enabling routine condensed-phase pulse radiolysis-TRIR measurements.**

External-cavity QCLs are extremely versatile, compact lasers that emit with a very narrow linewidth and can be continuously tuned over a wide range, often more than ± 50 cm⁻¹ of their center frequency.⁸⁴ In an EC-QCL, one of the facets of the QCL chip is anti-reflection coated, thus defeating the optical cavity action of the cleaved facets. A collimating lens and a diffraction grating, typically in a Littrow configuration, are arranged external to the QC chip to create the optical cavity. This reduces the laser emission to a single wavelength, which can then be tuned by simply rotating the grating. Commercial EC-QCLs are currently available at various center wavelengths ranging from 4.2 to 11.5 μm .⁸² The utility of EC-QCLs has already been demonstrated in IR spectroscopic studies of gas-phase and solid samples^{85–88} and in preliminary TRIR studies of solutions following laser flash photolysis.⁸⁹ It is therefore clear that they offer a unique combination of high output power, narrow line width, and wide, continuous tunability for use as an IR source in pulse radiolysis-TRIR applications.

In this paper we describe the first coupling of pulse radiolysis and nanosecond-TRIR spectroscopy to measurements in the condensed phase. The experiments were performed at the Laser-Electron Accelerator Facility (LEAF)⁴⁰ at Brookhaven National Laboratory (BNL), using two continuous wave EC-QCLs as IR probe sources. High quality TRIR kinetic traces were obtained on a near single-shot basis at multiple wavelengths across the tuning ranges of the EC-QCLs in order to build up TRIR spectra. We exemplify this approach by monitoring the pulse radiolytic formation of the one-electron reduced rhenium complex $[\text{Re}^{\text{I}}(\text{bpy}^*)(\text{CO})_3(\text{CH}_3\text{CN})]^0$ (bpy = 2,2'-bipyridyl) from $[\text{Re}^{\text{I}}(\text{bpy})(\text{CO})_3(\text{CH}_3\text{CN})]^+$ in acetonitrile and its subsequent decay. $[\text{Re}^{\text{I}}(\text{bpy})(\text{CO})_3(\text{CH}_3\text{CN})]^+$ has been shown to act as a catalyst for the photocatalytic reduction of CO₂ to CO in the presence of sacrificial electron donors, such as tertiary amines, and other rhenium complexes as photosensitizers,⁹⁰ and the one-electron reduced species is a key intermediate.

EXPERIMENTAL

Electron Pulse Generation. The LEAF facility at BNL led the application of photocathode electron gun accelerator

technology to picosecond pulse radiolysis studies of chemical kinetics and has been described in detail previously.⁴⁰ Briefly, in the normal operating mode of LEAF, 1–6 ps pulses of 266 nm laser light are used to excite photoelectrons from a magnesium photocathode housed inside a 30 cm long resonant cavity, radio frequency (RF) gun. The emitted electrons are then accelerated to ~9 MeV by a ~15 MW pulse of RF power from a klystron. Since the laser pulse is synchronized with the RF power to produce the electron pulse near the peak field gradient, the electron pulse length and intensity are a function of the laser pulse properties. Therefore, electron pulses as short as 5–7 ps with a typical charge of 5 nC are attainable (corresponding to a dose of ~30 Gy in a 1 cm aqueous sample). These processes are typically probed by UV, visible, or NIR transient absorption spectroscopy on the few picosecond timescale using a pulse-probe delay line⁴⁰ or optical fiber single-shot methodology³ or on the hundreds of picoseconds to microseconds timescale by direct transient-digitization of the signals from fast risetime detectors. However, in LEAF's alternative "macropulse" mode of operation, the photocathode is irradiated by ~5 ns 266 nm laser pulses (Spectra Physics, LAB-170), resulting in ~5 ns pulse width, 9 MeV electron pulses, which have approximately an order of magnitude greater radiolytic dose than the picosecond pulses. LEAF's macropulse is therefore ideally suited to TRIR experiments, and furthermore, the 5 ns pulse width conveniently matches the rise times of the fastest available mid-IR detectors ($\leq \sim 10$ ns).

Infrared Beam Geometry and Data Acquisition. Two continuous wave EC-QCLs were obtained from Daylight Solutions Inc. (Poway, CA),⁸² which were continuously tunable in the regions 1890–1960 cm^{-1} (Model 21052-MHF; 40 mW at gain center) and 1996–2084 cm^{-1} (Model 21049-MHF; <100 mW at gain center).[†] The Littrow configuration of the external cavity provides a narrow linewidth ($\sim 0.003 \text{ cm}^{-1}$) and mode-hop-free tuning. The output power of the lasers varies as a function of wavelength, dropping to zero at the extremities of the tuning range and peaking near the center. In the regular UV/visible transient absorption pulse radiolysis experiments at LEAF, the sample is housed inside an aluminum sample block at the end of the electron beamline in order to reduce RF pick-up by the detector electronics. A Faraday cup attached to the back of this housing is used to measure the charge dose in each electron pulse. The probe light (typically from a pulsed xenon lamp inside the accelerator vault), is focused into the sample and imaged through a hole in the wall onto a detector in the adjacent room. Extremely thin mirrors (aluminum-coated 0.5 mm thick silica substrate) inside the sample block transmit the electron beam with minimal scattering, permitting a reverse collinear beam geometry to maximize overlap of the electron and probe light beams in the sample and minimize collection of Cerenkov light generated in the sample by the electron beam. For the TRIR experiments reported here, we made use of the same sample housing block and some of the existing beam collection optics, with a few modifications. The two EC-QCLs were interchangeably mounted on a separate optical table inside the accelerator vault, ~4 m from the sample. Using aluminum mirrors, the IR

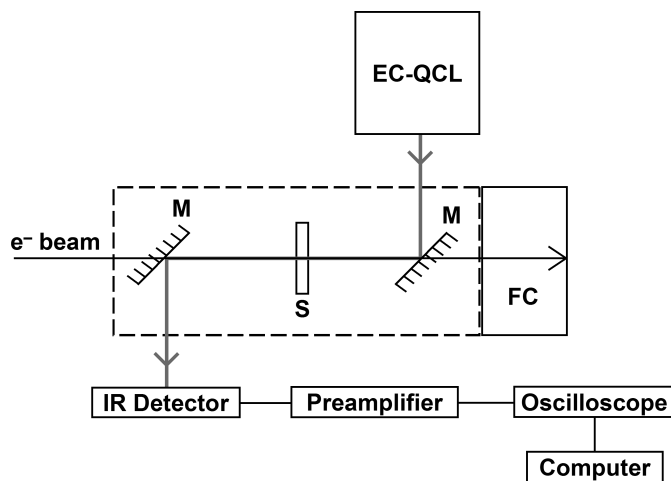


Fig. 1. Schematic representation of the beam geometry around the sample and the detection electronics used in the pulse radiolysis-TRIR experiments at LEAF (not shown to scale, and focusing and other optics not shown). Dashed line is the aluminum sample block housing and gray line is the IR beam. (EC-QCL) External-cavity quantum cascade laser; (FC) Faraday cup; (M) 0.5 mm thick aluminum-coated mirror; and (S) sample (IR flow cell).

beam was steered and focused through the sample and then guided another 4.5 m into the adjacent room, where it was refocused onto a liquid N_2 -cooled HgCdTe photovoltaic IR detector (Kolmar Technologies, Inc., KMPV11-1-LJ2/239) by a CaF_2 lens (20 cm focal length). The IR detector is equipped with a built-in 20 MHz preamplifier with AC- and DC-coupled outputs and has a response time of <20 ns. Due to the high output power of the EC-QCLs, it was necessary to attenuate the IR beam with neutral density filters at some IR frequencies in order to avoid saturation of the detector's preamplifier. The signals from the detector were digitized by the regular LEAF data collection oscilloscope (LeCroy WaveMaster 8620A, 6 GHz),[‡] with data acquisition being controlled by custom LabVIEW software. Figure 1 shows a schematic diagram of the experimental setup for pulse radiolysis-TRIR. It should be noted that since we were working in the 5 μm region of the mid-IR, where atmospheric water absorptions are less problematic, it was not necessary to transport the IR beam through purged tubing. TRIR kinetic traces were acquired on a point-by-point basis by tuning the EC-QCLs across their tuning ranges in steps of approximately 2 to 4 cm^{-1} . For each trace, I_0 measurements of the IR light level were made before pulse radiolysis using the DC-coupled output of the detector's preamplifier, and transient measurements after pulse radiolysis were made using the AC-coupled output. Conversion to ΔOD kinetic traces was achieved with Eq. 1, where AC represents the raw kinetic trace from the AC-coupled output, and the factor of two accounts for the fact that the transimpedance amplification of the detector's AC signal is twice that of its DC signal:

$$\Delta\text{OD} = -\log_{10} \left(1 + \frac{\text{AC}}{2I_0} \right) \quad (1)$$

[†] EC-QCL technology continues to improve and the current versions of our lasers now cover an even broader range (up to 140 cm^{-1} each), with no tuning gap between the two lasers. Indeed, one of our EC-QCLs has recently been modified by Daylight Solutions to widen its tuning range to 1872–1978 cm^{-1} .

[‡] Such a high bandwidth oscilloscope is not required for nanosecond TRIR measurements, but was used to minimize disruption to the regular LEAF data acquisition setup.

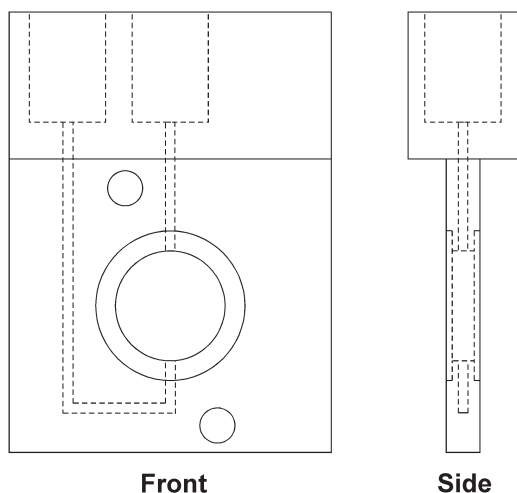


FIG. 2. Front and side views of the stainless steel body (1.1-in. w \times 1.5-in. h) of the miniature home-built IR flow cell used in the pulse radiolysis-TRIR experiments at LEAF. Dashed lines represent internal holes and recesses.

Igor Pro software was used to assemble TRIR spectra from the combined traces and for kinetic analysis.

Sample Handling. $[\text{Re}^{\text{I}}(\text{bpy})(\text{CO})_3(\text{CH}_3\text{CN})]^+[\text{PF}_6]^-$ was prepared according to a literature procedure.⁹¹ Acetonitrile (Aldrich, anhydrous) was degassed with argon, stored in a glovebox, and used without further purification. For a typical experiment, 20 mL of a 1.5 mM acetonitrile solution of $[\text{Re}^{\text{I}}(\text{bpy})(\text{CO})_3(\text{CH}_3\text{CN})]^+[\text{PF}_6]^-$ was prepared in the glovebox, where it was transferred into a special glass reservoir vessel fitted with glass-to-kovar metal tube seals, Swagelok fittings, and Teflon valves. The reservoir vessel was then connected to a vacuum-tight flow system that has a connection to a vacuum/gas manifold. Due to size constraints within the LEAF sample housing block, it was necessary to construct a miniature IR flow cell (see Fig. 2). This consists of a 1.1-in. w \times 1.5-in. h stainless steel plate with a 3/8-in. ϕ hole drilled through the center. Recessed shoulders surround the hole on either side of the plate to accommodate two 0.5-in. $\phi \times 0.5$ mm thick sapphire windows. Holes with an inner diameter of 1/32 in. are drilled through the steel plate to allow liquid to be flowed through the cell (dashed lines in Fig. 2) via standard flat-bottom 1/4-28 threaded ports at the top of the cell. Thin Teflon gaskets (~ 100 μm) are placed on the recessed shoulders to provide a seal for the sapphire windows, which are clamped tightly in place using Thorlabs SM05-threaded cage plates (P/N: SP02) on either side of the cell, which are themselves bolted together via two through-holes. The design of the cell body resulted in a fixed path length of 2 mm and tests showed that the assembled cell was vacuum-tight. The remainder of the flow system consisted of 1/16-in. PEEK tubing and a recirculating gear pump (Micropump). The flow system tubing was evacuated and refilled with argon to a pressure of 2 atm at least three times before sealing the flow system and circulating the solution cyclically through the flow cell for the TRIR experiment.

Step-Scan Fourier Transform Infrared Spectroscopy. Time-resolved step-scan FT-IR experiments with pulsed 355 nm laser excitation were performed on a Bruker IFS 66/S apparatus that has previously been described in detail.⁹² The same flow system as described above was used, but with a

commercially available CaF_2 IR flow cell (Harrick Scientific Products, DLC-S25).

RESULTS AND DISCUSSION

Infrared Cell Window Material and Sensitivity of the Pulse Radiolysis-Time-Resolved Infrared Apparatus. Our goal was to demonstrate acquisition of TRIR kinetic traces on the nanosecond timescale following pulse radiolysis of condensed-phase samples, on a single- or near single-shot basis. Single-shot sensitivity is necessary since the LEAF accelerator operates at a low repetition rate (typically ≤ 1 Hz during this kind of automated data acquisition) and samples subjected to pulse radiolysis are gradually decomposed by the electron pulses. It was first necessary to find a suitable window material that would transmit mid-IR light without generating artifacts in the transient IR signals recorded after pulse radiolysis. We performed TRIR tests on an empty KBr cavity cell (Spectra-Tech, Inc.; P/N: Z11231-3; 10 mm total thickness of KBr), on two 2 mm thick CaF_2 windows, and on two 0.5 mm thick sapphire windows. Kinetic traces were recorded in emission mode (i.e., by recording the signal intensity from the AC-coupled detector output without IR probe light) following pulse radiolysis of the different window materials placed inside the LEAF sample housing block.

For the KBr cavity cell, a large transient emission signal was produced immediately upon pulse radiolysis, decaying with a lifetime of ~ 50 ns. In addition, the cell developed intense blue color centers. Better results were obtained with the CaF_2 windows, with the radiation-induced IR emission signal being approximately eight times smaller. However, faint color centers in the window were observed after a short period of pulse radiolysis. The best results were obtained with the sapphire windows, which produced negligible IR emission upon pulse radiolysis and no detectable color centers. Since 0.5 mm thick sapphire has sufficient transmittance in the 5 μm region, we used the sapphire windows in the IR flow cell for the TRIR measurements.

To test the sensitivity of the new TRIR apparatus, we tuned one of the EC-QCLs to an IR frequency near the center of its tuning range (1938 cm^{-1}) and recorded a TRIR kinetic absorption trace with the empty IR flow cell in the sample housing block. This trace was obtained as the average of four individual traces and it is clear from Fig. 3 that TRIR signal levels on the order of $\Delta\text{OD} < 1 \times 10^{-3}$ can easily be detected with this apparatus following pulse radiolysis, on a near single-shot basis.

Time-Resolved Infrared Spectroscopy Following Pulse Radiolysis of $[\text{Re}^{\text{I}}(\text{bpy})(\text{CO})_3(\text{CH}_3\text{CN})]^+$ in Acetonitrile. The reduction of CO_2 into renewable fuels and chemicals is an important field of research, since using CO_2 captured from industrial emissions may help to mitigate the effects of global warming and our dwindling supplies of fossil fuels.^{93,94} Unfortunately, being the final product of combustion, CO_2 is an extremely stable molecule, requiring large amounts of energy and the use of special catalysts to convert it into reduced forms. Using sunlight to drive these reactions in so-called “artificial photosynthetic” processes is an extremely attractive option, since it is a plentiful and clean source of energy; more energy strikes the earth from the Sun in one hour than an entire year’s worth of global energy consumption. However, developing catalysts that can efficiently harness solar energy and promote multi-electron CO_2 reduction reactions is paramount to the success of such a strategy.

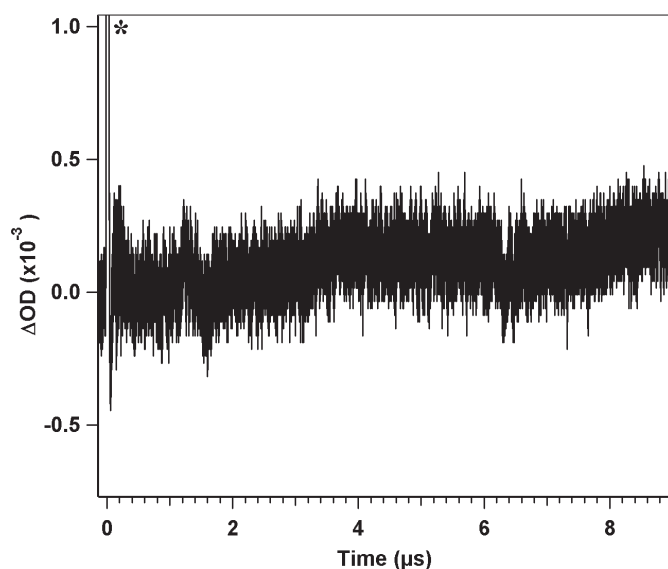


FIG. 3. EC-QCL TRIR kinetic trace recorded at 1938 cm^{-1} after pulse radiolysis of the empty sapphire window IR flow cell. (*) Small transient absorption signal (FWHM $\sim 30\text{ ns}$) that gradually builds up on the signal with prolonged use of the same sapphire windows.

$[\text{Re}^{\text{I}}(\text{bpy})(\text{CO})_3(\text{CH}_3\text{CN})]^+$ has previously been shown to act as a catalyst in the photocatalytic reduction of CO_2 to CO in the presence of sacrificial electron donors (e.g., triethanolamine or triethylamine) and another rhenium complex as a photosensitizer.⁹⁰ Its one-electron reduced form, $[\text{Re}^{\text{I}}(\text{bpy}^{\bullet-})(\text{CO})_3(\text{CH}_3\text{CN})]^0$ is a key intermediate in the catalytic cycle. However, the precise mechanism of its reactivity following the reduction step remains unknown and pulse radiolysis offers a unique opportunity to investigate this reactivity in the absence of sacrificial electron donors. Therefore, in a preliminary effort to determine whether we can monitor the formation of the one-electron reduced species by TRIR following pulse radiolysis, we performed pulse radiolysis with TRIR detection on $[\text{Re}^{\text{I}}(\text{bpy})(\text{CO})_3(\text{CH}_3\text{CN})]^+$ in argon-saturated acetonitrile, using LEAF's macropulse for excitation. This was also a convenient system with which to demonstrate the pulse radiolysis-TRIR experiment because we could easily characterize the one-electron reduced intermediate in a separate laser flash photolysis TRIR experiment, allowing a direct comparison with the pulse radiolysis experiment (see below).

It has already been established that pulse radiolysis of acetonitrile solutions results in highly reducing conditions due to the formation of an equilibrium mixture of solvated electrons (consisting of an electron trapped in a cavity of several CH_3CN molecules) and the acetonitrile radical anion dimer, $(\text{CH}_3\text{CN})_2^{\bullet-}$.⁹⁵ Thus, since acetonitrile is also suitably transparent in the $\nu(\text{CO})$ IR region, it is an ideal solvent for our TRIR measurements. Figure 4a shows three TRIR spectra recorded in the $\nu(\text{CO})$ region at time delays of 80 ns, 3.1 μs , and 13 μs after pulse radiolysis of $[\text{Re}^{\text{I}}(\text{bpy})(\text{CO})_3(\text{CH}_3\text{CN})]^+$ in argon-saturated acetonitrile. Bleaching of the two ground state $\nu(\text{CO})$ IR bands at 1936 and 2040 cm^{-1} is clearly observed, together with an instantaneous formation of two new transient bands shifted to lower wavenumbers at 1904 and 2014 cm^{-1} . It was not possible to cover the regions between the transient bands and on the low-frequency side of the 1904 cm^{-1} band due to the available tuning ranges of our EC-QCLs. The red-shift of the $\nu(\text{CO})$ bands of the transient species relative to the ground state is characteristic of the

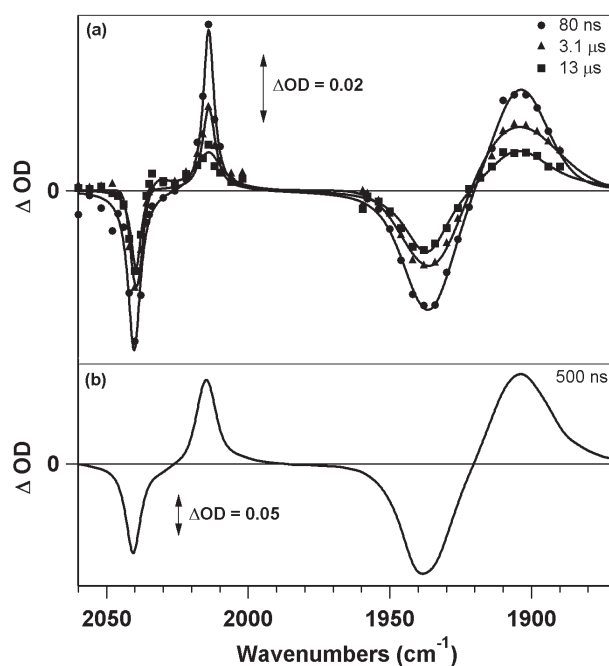


FIG. 4. (a) EC-QCL TRIR spectra recorded at the specified time delays after pulse radiolysis of $1.5\text{ mM } [\text{Re}^{\text{I}}(\text{bpy})(\text{CO})_3(\text{CH}_3\text{CN})]^+$ in acetonitrile saturated with 2 atm of argon. Smooth lines are multi-peak Voigt curve fits of the data. (b) Time-resolved step-scan FT-IR spectrum recorded 500 ns after 355 nm laser flash photolysis of $1.4\text{ mM } [\text{Re}^{\text{I}}(\text{bpy})(\text{CO})_3(\text{CH}_3\text{CN})]^+$ in acetonitrile saturated with 2 atm of argon, in the presence of 0.5 M triethylamine as a sacrificial electron donor. This is the original step-scan FT-IR spectrum (not curve-fitted).

formation of the one-electron reduced complex, $[\text{Re}^{\text{I}}(\text{bpy}^{\bullet-})(\text{CO})_3(\text{CH}_3\text{CN})]^0$, in which there is increased electron density at the rhenium center, resulting in more π -back bonding into the π^* anti-bonding orbitals of the CO ligands and a weakening of the $\text{C}\equiv\text{O}$ bonds. It has previously been shown that the extra electron in the one-electron reduced form of this type of rhenium complex resides in the π^* anti-bonding orbitals of the bpy ligand.⁹⁶ By comparing the intensities of the bleach bands in the TRIR spectrum recorded immediately after pulse radiolysis ($\Delta t = 35\text{ ns}$) with those of the IR bands of the ground state before pulse radiolysis, we estimate that each electron pulse generates $\sim 55\text{ }\mu\text{M}$ of reduced complex.

To confirm that the TRIR spectra observed after pulse radiolysis are due to the expected reduction product, we performed a laser flash photolysis TRIR experiment on $[\text{Re}^{\text{I}}(\text{bpy})(\text{CO})_3(\text{CH}_3\text{CN})]^+$ in acetonitrile in the presence of 0.5 M triethylamine (TEA) as a sacrificial electron donor. Photoexcitation of the rhenium complex into its metal-to-ligand charge transfer (MLCT) excited state results in rapid reductive quenching by electron transfer from TEA, forming the long-lived (on the order of seconds) reduced complex, $[\text{Re}^{\text{I}}(\text{bpy}^{\bullet-})(\text{CO})_3(\text{CH}_3\text{CN})]^0$.⁹⁷ Figure 4b shows a time-resolved step-scan FT-IR spectrum from this experiment, recorded 500 ns after 355 nm laser excitation. The spectrum is almost identical to the pulse radiolysis-TRIR spectra apart from the intensity ratio of the high- and low-frequency $\nu(\text{CO})$ bands, which is likely a result of the different spectral resolutions in the two experiments, thus supporting our interpretation of the pulse radiolysis-TRIR data.

In the pulse radiolysis experiment, the two transient bands decay and the two bleach bands recover to $\sim 15\%$ and $\sim 35\%$ of their initial intensities, respectively, on the $90\text{ }\mu\text{s}$ timescale

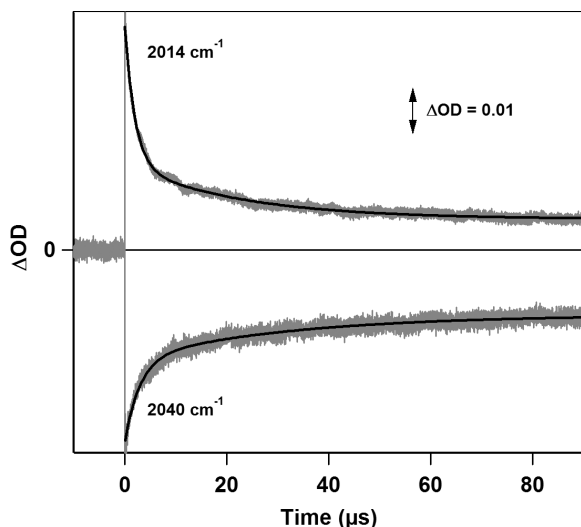


FIG. 5. TRIR kinetic traces recorded at 2014 and 2040 cm^{-1} after pulse radiolysis of 1.5 mM $[\text{Re}^{\text{I}}(\text{bpy})(\text{CO})_3(\text{CH}_3\text{CN})]^+$ in acetonitrile saturated with 2 atm of argon. Black curves are bi-exponential fits of the data.

(see Fig. 5). The kinetic decay traces clearly exhibit bi-exponential behavior, with the average lifetimes of the two components of the transient decay being $\tau_1 = 2.4 \pm 0.2 \mu\text{s}$ and $\tau_2 = 23.0 \pm 3 \mu\text{s}$ and those of the bleach recovery being $\tau_1 = 2.8 \pm 0.3 \mu\text{s}$ and $\tau_2 = 28.8 \pm 3 \mu\text{s}$. This was unexpected, since the one-electron reduced species prepared by electro- or photochemical methods is stable on the seconds timescale. However, it is likely that in the pulse radiolysis experiment the one-electron reduced complex is oxidized by various cations and radicals present in solution, particularly by $\text{CH}_3\text{CN}^{+\bullet}$, resulting in a faster recovery of the starting complex by more than one possible pathway. Future experiments will examine the radiolytic dose dependence of the decay kinetics, together with the possible use of additives that will scavenge the $\text{CH}_3\text{CN}^{+\bullet}$ cations (e.g., aniline).⁹⁸ Since the reaction of the related one-electron reduced complex $[\text{Re}^{\text{I}}(\text{dmb}^{\bullet})(\text{CO})_3(\text{CH}_3\text{CN})]^0$ (dmb = 4,4'-dimethyl-2,2'-bipyridine) in acetonitrile with CO_2 is known to be very slow,⁹⁷ future work will also involve the use of the pulse radiolysis-TRIR technique to investigate the reactivity of other rhenium complexes (synthetically modified for solubility in alkanes), toward CO_2 in isooctane solution following one-electron reduction. This would be aided by the use of more EC-QCLs covering a wider region of the mid-IR.

CONCLUSION

Pulse radiolysis is an extremely powerful method for rapidly generating one-electron reduced and oxidized species and probing their subsequent reactivity with time-resolved spectroscopic methods. However, transient detection has been mainly limited to the UV/visible/NIR regions, where structural information on the species being probed is often lacking in the spectra. TRIR spectroscopy offers the structural specificity that is lacking and is applicable to a wide array of samples, but until now it has only been used to study a few gas-phase reactions following pulse radiolysis, due to several technical challenges.

Taking advantage of recent technological developments in IR laser technology in the form of high-power, continuous-wave,

tunable external-cavity quantum cascade lasers, we have constructed a nanosecond TRIR detection apparatus for the investigation of condensed-phase samples subjected to excitation by pulse radiolysis. This is the first demonstration of fast TRIR detection following pulse radiolysis of condensed-phase systems. Using two EC-QCLs we were able to cover a probe region spanning 1890–2084 cm^{-1} , which could easily be expanded in the future through the purchase of a suite of additional EC-QCLs and/or a CO gas laser. The sensitivity of the apparatus is on the order of $\Delta\text{OD} < 1 \times 10^{-3}$ (after four averaged shots), with a response time of $< 20 \text{ ns}$. A preliminary TRIR experiment has demonstrated its utility for obtaining high quality TRIR spectral and kinetic data on the nanosecond timescale following pulse radiolysis, by monitoring the formation and decay of the one-electron reduced CO_2 reduction photocatalyst $[\text{Re}^{\text{I}}(\text{bpy}^{\bullet})(\text{CO})_3(\text{CH}_3\text{CN})]^0$ in acetonitrile solution.

Since TRIR spectroscopy offers rich information about the structures of transient species, the availability of routine TRIR spectroscopic detection for pulse radiolysis now opens up the possibility of studying the mechanisms of a wide range of redox processes that were previously difficult, or even impossible, to study with time-resolved UV/visible detection methods. Examples include unraveling the mechanistic reactivity of biologically important nitrogen oxide species such as nitroxyl (HNO) and NO^- , which lack any UV/visible absorption bands, and the investigation of transition metal-based redox catalysts for solar energy conversion and other catalytic applications. The identification of transient intermediates following the radiolysis of ionic liquids and conventional solvents, which will be critical for the development of advanced nuclear fuel cycles, will also be greatly aided by the application of TRIR methods following pulse radiolysis.

ACKNOWLEDGMENTS

This work was performed at Brookhaven National Laboratory and was funded under contract DE-AC02-98CH10886 with the U.S. Department of Energy and supported by its Division of Chemical Sciences, Geosciences & Biosciences, Office of Basic Energy Sciences. We are grateful for discussions with Dr. Sergei Lymar (BNL) regarding possible pulse radiolysis-TRIR experiments with HNO and NO^- . MWG gratefully acknowledges the receipt of a Royal Society Wolfson Merit Award.

1. R. G. W. Norrish and G. Porter, *Nature (London)* **164**, 658 (1949).
2. G. R. Fleming, *Chemical Applications of Ultrafast Spectroscopy* (Oxford University Press, Oxford, 1986).
3. A. R. Cook and Y. Z. Shen, *Rev. Sci. Instrum.* **80**, 073106 (2009).
4. K. Henbest and M. A. J. Rodgers, "Photochemical Techniques", in *Electron Transfer in Chemistry*, M. A. J. Rodgers, Ed. (Wiley-VCH, Weinheim, 2001), vol. 1, p. 558.
5. S. T. Roberts, K. Ramasesha, and A. Tokmakoff, *Acc. Chem. Res.* **42**, 1239 (2009).
6. J. R. Schoonover and G. F. Strouse, *Chem. Rev.* **98**, 1335 (1998).
7. K. McFarlane, B. Lee, J. Bridgewater, and P. C. Ford, *J. Organomet. Chem.* **554**, 49 (1998).
8. D. C. Grills and M. W. George, "Fast and Ultrafast Time-Resolved Mid-Infrared Spectrometry Using Lasers", in *Handbook of Vibrational Spectroscopy*, J. M. Chalmers and P. R. Griffiths, Eds. (John Wiley and Sons, Chichester, 2002), vol. 1, pp. 677–692.
9. B. Chance, *Rev. Sci. Instrum.* **22**, 619 (1951).
10. M. S. Hargrove, "Ligand Binding with Stopped-Flow Rapid Mixing", in *Protein-Ligand Interactions: Methods and Applications*, G. U. Nienhaus, Ed. (Humana Press, Totowa, 2005), pp. 323–341.
11. J. V. Beitz, G. W. Flynn, D. H. Turner, and N. Sutin, *J. Am. Chem. Soc.* **92**, 4130 (1970).
12. R. B. Dyer, F. Gai, and W. H. Woodruff, *Acc. Chem. Res.* **31**, 709 (1998).
13. M. Gruebele, J. Sabelko, R. Ballew, and J. Ervin, *Acc. Chem. Res.* **31**, 699 (1998).
14. S. V. Lymar and J. K. Hurst, *J. Am. Chem. Soc.* **117**, 8867 (1995).

15. L. K. Patterson, "Instrumentation for Measurement of Transient Behavior in Radiation Chemistry", in *Radiation Chemistry: Principles and Applications*, Farhataziz and M. A. J. Rodgers, Eds. (VCH, New York, 1987), pp. 65–96.
16. Y. Tabata, *Pulse Radiolysis* (CRC Press, Boca Raton, FL, 1990).
17. J. F. Wishart, "Accelerators for Ultrafast Phenomena", in *Radiation Chemistry: Present Status and Future Trends*, C. D. Jonah and B. S. M. Rao, Eds. (Elsevier Science, Amsterdam, 2001), vol. 87, pp. 21–35.
18. C. Creutz, H. A. Schwarz, J. F. Wishart, E. Fujita, and N. Sutin, *J. Am. Chem. Soc.* **113**, 3361 (1991).
19. E. Fujita, J. F. Wishart, and R. van Eldik, *Inorg. Chem.* **41**, 1579 (2002).
20. D. E. Polyansky, D. Cabelli, J. T. Muckerman, T. Fukushima, K. Tanaka, and E. Fujita, *Inorg. Chem.* **47**, 3958 (2008).
21. J. F. Wishart and I. A. Shkrob, "The Radiation Chemistry of Ionic Liquids and its Implications for their use in Nuclear Fuel Processing", in *ACS Symposium Series Vol. 1030: Ionic Liquids: From Knowledge to Application*, N. V. Plechkova, R. D. Rogers, and K. R. Seddon, Eds. (American Chemical Society, Washington, D.C., 2009), pp. 119–134.
22. S. Asaoka, N. Takeda, T. Lyoda, A. R. Cook, and J. R. Miller, *J. Am. Chem. Soc.* **130**, 11912 (2008).
23. M. Adinarayana, E. Bothe, and D. Schulte-Frohlinde, *Int. J. Radiat. Biol.* **54**, 723 (1988).
24. S. Steenken, *Chem. Rev.* **89**, 503 (1989).
25. S. Steenken, S. V. Jovanovic, M. Bietti, and K. Bernhard, *J. Am. Chem. Soc.* **122**, 2373 (2000).
26. O. V. Gerasimov and S. V. Lymar, *Inorg. Chem.* **38**, 4317 (1999).
27. L. J. Hayward, J. A. Rodriguez, J. W. Kim, A. Tiwari, J. J. Goto, D. E. Cabelli, J. S. Valentine, and R. H. Brown, *J. Biol. Chem.* **277**, 15923 (2002).
28. G. V. Buxton, "An overview of the radiation chemistry of liquids", in *Radiation Chemistry: From Basics to Applications in Material and Life Sciences*, M. Spothem-Maurizot, M. Mostafavi, T. Douki, and J. Belloni, Eds. (EDP Sciences, Les Ulis, France, 2008), pp. 3–16.
29. Comment made by M. Sangster on p. 112 of *Discuss. Faraday Soc.* **17**, 90 (1954).
30. J. P. Keene, *Nature (London)* **188**, 843 (1960).
31. M. S. Matheson and L. M. Dorfman, *J. Chem. Phys.* **32**, 1870 (1960).
32. R. L. McCarthy and A. MacLachlan, *Trans. Faraday Soc.* **56**, 1187 (1960).
33. E. J. Hart and J. W. Boag, *J. Am. Chem. Soc.* **84**, 4090 (1962).
34. R. H. Schuler, *Radiat. Phys. Chem.* **43**, 417 (1994).
35. R. H. Schuler, *Radiat. Phys. Chem.* **47**, 9 (1996).
36. A. D. Trifunac, R. G. Lawler, D. M. Bartels, and M. C. Thurnauer, *Prog. React. Kinet.* **14**, 43 (1986).
37. I. A. Shkrob and A. D. Trifunac, *Radiat. Phys. Chem.* **50**, 227 (1997).
38. D. W. Werst and A. D. Trifunac, *Acc. Chem. Res.* **31**, 651 (1998).
39. F. C. Grozema, R. Hoofman, L. P. Candea, M. P. de Haas, J. M. Warman, and L. D. A. Siebbeles, *J. Phys. Chem. A* **107**, 5976 (2003).
40. J. F. Wishart, A. R. Cook, and J. R. Miller, *Rev. Sci. Instrum.* **75**, 4359 (2004).
41. A. Saeiki, T. Kozawa, S. Kashiwagi, K. Okamoto, G. Isoyama, Y. Yoshida, and S. Tagawa, *Nucl. Instrum. Methods Phys. Res., Sect. A* **546**, 627 (2005).
42. R. F. Dallinger, J. J. Guanci, W. H. Woodruff, and M. A. J. Rodgers, *J. Am. Chem. Soc.* **101**, 1355 (1979).
43. N. H. Jensen, R. Wilbrandt, P. B. Pagsberg, A. H. Sillesen, and K. B. Hansen, *J. Am. Chem. Soc.* **102**, 7441 (1980).
44. R. Wilbrandt and N. H. Jensen, *J. Am. Chem. Soc.* **103**, 1036 (1981).
45. G. N. R. Tripathi, *J. Chem. Phys.* **74**, 6044 (1981).
46. G. N. R. Tripathi and R. H. Schuler, *J. Chem. Phys.* **81**, 113 (1984).
47. G. N. R. Tripathi and R. H. Schuler, *Chem. Phys. Lett.* **110**, 542 (1984).
48. G. N. R. Tripathi, S. Qun, D. A. Armstrong, D. M. Chipman, and R. H. Schuler, *J. Phys. Chem.* **96**, 5344 (1992).
49. G. N. R. Tripathi and Y. L. Su, *J. Phys. Chem. A* **108**, 3478 (2004).
50. R. Wilbrandt, N. H. Jensen, P. Pagsberg, A. H. Sillesen, K. B. Hansen, and R. E. Hester, *Chem. Phys. Lett.* **60**, 315 (1979).
51. Y. L. Su and G. N. R. Tripathi, *Chem. Phys. Lett.* **188**, 388 (1992).
52. H. A. Schwarz, *J. Chem. Phys.* **67**, 5525 (1977).
53. H. A. Schwarz, *J. Chem. Phys.* **72**, 284 (1980).
54. J. T. Jodkowski, E. Ratajczak, A. Sillesen, and P. Pagsberg, *Chem. Phys. Lett.* **203**, 490 (1993).
55. A. Sillesen, E. Ratajczak, and P. Pagsberg, *Chem. Phys. Lett.* **201**, 171 (1993).
56. H. Meunier, P. Pagsberg, and A. Sillesen, *Chem. Phys. Lett.* **261**, 277 (1996).
57. P. Pagsberg, A. Sillesen, J. T. Jodkowski, and E. Ratajczak, *Chem. Phys. Lett.* **252**, 165 (1996).
58. P. Pagsberg, A. Sillesen, J. T. Jodkowski, and E. Ratajczak, *Chem. Phys. Lett.* **249**, 358 (1996).
59. P. Pagsberg, E. Bjergbakke, E. Ratajczak, and A. Sillesen, *Chem. Phys. Lett.* **272**, 383 (1997).
60. P. Pagsberg, J. T. Jodkowski, E. Ratajczak, and A. Sillesen, *Chem. Phys. Lett.* **286**, 138 (1998).
61. S. Le Caër, G. Vigneron, J. P. Renault, and S. Pommeret, *Chem. Phys. Lett.* **426**, 71 (2006).
62. S. Le Caër, G. Vigneron, J. P. Renault, and S. Pommeret, *Radiat. Phys. Chem.* **76**, 1280 (2007).
63. T. Yuzawa, C. Kato, M. W. George, and H. O. Hamaguchi, *Appl. Spectrosc.* **48**, 684 (1994).
64. S. Srivastava, J. P. Toscano, R. J. Moran, and D. E. Falvey, *J. Am. Chem. Soc.* **119**, 11552 (1997).
65. M. Poliakoff and E. Weitz, *Adv. Organomet. Chem.* **25**, 277 (1986).
66. M. W. George, M. Poliakoff, and J. J. Turner, *Analyst* **119**, 551 (1994).
67. W. Uhmann, A. Becker, C. Taran, and F. Siebert, *Appl. Spectrosc.* **45**, 390 (1991).
68. P. Y. Chen and R. A. Palmer, *Appl. Spectrosc.* **51**, 580 (1997).
69. J. Faist, F. Capasso, D. L. Sivco, C. Sirtori, A. L. Hutchinson, and A. Y. Cho, *Science (Washington, D.C.)* **264**, 553 (1994).
70. C. Gmachl, F. Capasso, D. L. Sivco, and A. Y. Cho, *Rep. Prog. Phys.* **64**, 1533 (2001).
71. A. A. Kosterev and F. K. Tittel, *IEEE J. Quant. Electron.* **38**, 582 (2002).
72. G. Wysocki, A. A. Kosterev, and F. K. Tittel, *Appl. Phys. B-Lasers Opt.* **80**, 617 (2005).
73. A. A. Kosterev, A. L. Malinovsky, F. K. Tittel, C. Gmachl, F. Capasso, D. L. Sivco, J. N. Baillargeon, A. L. Hutchinson, and A. Y. Cho, *Appl. Opt.* **40**, 5522 (2001).
74. Y. A. Bakhrkin, A. A. Kosterev, C. Roller, R. F. Curl, and F. K. Tittel, *Appl. Opt.* **43**, 2257 (2004).
75. J. P. Lima, H. Vargas, A. Miklos, M. Angelmahr, and P. Hess, *Appl. Phys. B-Lasers Opt.* **85**, 279 (2006).
76. H. Ganser, M. Horstjann, C. V. Suschek, P. Hering, and M. Murtz, *Appl. Phys. B-Lasers Opt.* **78**, 513 (2004).
77. B. Lendl, J. Frank, R. Schindler, A. Muller, M. Beck, and J. Faist, *Anal. Chem.* **72**, 1645 (2000).
78. W. B. Martin, S. Mirov, and R. Venugopalan, *Appl. Spectrosc.* **59**, 881 (2005).
79. A. Lambrecht, T. Beyer, K. Hebestreit, R. Mischler, and W. Petrich, *Appl. Spectrosc.* **60**, 729 (2006).
80. S. Schaden, A. Dominguez-Vidal, and B. Lendl, *Appl. Spectrosc.* **60**, 568 (2006).
81. S. Schaden, A. Dominguez-Vidal, and B. Lendl, *Appl. Phys. B-Lasers Opt.* **86**, 347 (2007).
82. <http://www.daylightsolutions.com>.
83. E. Takeuchi, K. Thomas, and T. Day, "Quantum Cascade Lasers: Applications multiply for external-cavity QCLs", in *Laser Focus World* (2009), vol. 45, Issue 1.
84. C. Peng, G. P. Luo, and H. Q. Le, *Appl. Opt.* **42**, 4877 (2003).
85. Q. Wen and K. H. Michaelian, *Opt. Lett.* **33**, 1875 (2008).
86. G. Wysocki, R. Lewicki, R. F. Curl, F. K. Tittel, L. Diehl, F. Capasso, M. Troccoli, G. Hofler, D. Bour, S. Corzine, R. Maulini, M. Giovannini, and J. Faist, *Appl. Phys. B-Lasers Opt.* **92**, 305 (2008).
87. A. Karpf and G. N. Rao, *Appl. Opt.* **48**, 5061 (2009).
88. C. W. Van Neste, L. R. Senesac, and T. Thundat, *Anal. Chem.* **81**, 1952 (2009).
89. J. A. Calladine and M. W. George, *Spectrosc. Eur.* **21**, 6 (2009).
90. H. Takeda, K. Koike, H. Inoue, and O. Ishitani, *J. Am. Chem. Soc.* **130**, 2023 (2008).
91. J. V. Caspar and T. J. Meyer, *J. Phys. Chem.* **87**, 952 (1983).
92. D. C. Grills, R. van Eldik, J. T. Muckerman, and E. Fujita, *J. Am. Chem. Soc.* **128**, 15728 (2006).
93. A. J. Morris, G. J. Meyer, and E. Fujita, *Acc. Chem. Res.* **42**, 1983 (2009).
94. M. D. Doherty, D. C. Grills, J. T. Muckerman, D. E. Polyansky, and E. Fujita, *Coord. Chem. Rev.*, paper in press (2010).
95. I. A. Shkrob and M. C. Sauer, *J. Phys. Chem. A* **106**, 9120 (2002).
96. T. Scheiring, A. Klein, and W. Kaim, *J. Chem. Soc.-Perkin Trans. 2*, 2569 (1997).
97. Y. Hayashi, S. Kita, B. S. Brunschwig, and E. Fujita, *J. Am. Chem. Soc.* **125**, 11976 (2003).
98. S. Nad and H. Pal, *J. Chem. Phys.* **116**, 1658 (2002).